# MODELLING OF FLOW PATHS IN A STRUCTURALLY-CONTROLLED BASIN, NGAKURU GRABEN, TAUPO VOLCNIC ZONE, NEW ZEALAND

W.M. Kissling[1], A.J. Rae[2], P. Villamor[3] and S.E. Ellis[3]

[1]Callaghan Innovation, P.O. Box 31310, Lower Hutt, New Zealand

[2]GNS Science, Private Bag 2000, Taupo, New Zealand

[3]GNS Science, P.O. Box 30368, Lower Hutt, New Zealand

w.kissling@gns.cri.nz

**Keywords:** *Ngakuru Graben, geothermal systems, silica sinter, hydrothermal alteration, fluid flow, modelling, TOUGH2*

## ABSTRACT

The Ngakuru Graben is bounded by the eastern Paeroa and western Ngakuru Faults. The structural fabric within the graben is characterised by northeast-trending normal faults, with opposing northwest- and southeast-facing faults defining the central rift axis. The geology of the graben is dominated by ignimbrite sequences that are overlain by lake sediments and Quaternary surface alluvium.

Surface expressions of geothermal activity occur on the graben margins, especially along the eastern and western boundaries, at Te Kopia, Waikite, Orakeikorako, Atiamuri, Ngapouri and Horohoro. Similarly, areas of extinct hydrothermal activity (i.e., silica sinter and hydrothermal eruption deposits, and hydrothermally-altered lake sediments) are also located marginal to the graben. Dating of organic material ($^{14}$C) in fossil sinter from various locations shows that hydrothermal activity has been ongoing in the area for at least the last 34 ± 0.5 ka.

The temporal and spatial characteristics of geothermal activity within the Ngakuru Graben raise important questions regarding the controls of fluid flow paths in a structurally controlled basin. What are the important parameters that influence permeability? Why is hydrothermal activity restricted to the margins of the graben, and why has activity at many of these geothermal areas been extinguished?

A TOUGH2 model of this system has been developed to address these questions. The simplified model represents a northwest-southeast section across the graben and contains four geological units - shallow and deep volcanics within the graben, a low permeability unit exterior to it and a high permeability unit associated with faulting at the graben margins.

We show that both upflows of warm water and downflows of cool surface waters can occur within these faults, and that these flows and the regional-scale flows within the graben can be controlled by small changes in the fault permeabilities. We discuss the dynamics of these upflows and how they might relate to the areas of hydrothermal activity observed at the basin margins.

## 1. INTRODUCTION

The Ngakuru Graben is a structurally-controlled basin within the extensional Taupo Fault Belt (Villamor and Berryman, 2001; Rowland and Sibson, 2001). It is located approximately 40 km north-northwest of Taupo township and 20 km southeast of Rotorua city. The basin has a northeast – southwest long orientation with the northwest boundary defined by the Ngakuru Fault and its southeast boundary by the Paeroa Fault. The basin is transected by northeast-trending normal faults, with opposing northwest- and southeast-facing faults defining a central rift axis along the Maleme Fault (Rowland and Sibson, 2001).

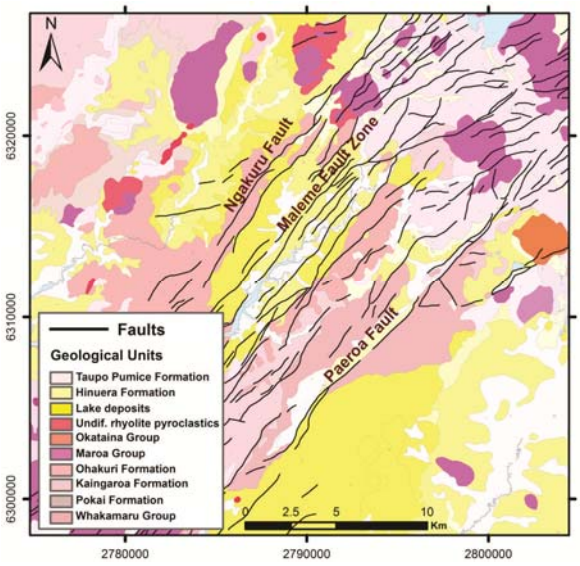


**Figure 1: Geology map of the Ngakuru Graben (Leonard et al., 2010).**

Surface geology of the basin is shown in Figure 1. Oldest rocks crop out in the southern and southeastern parts of the basin, with the Paeroa Ignimbrite (Whakamaru-group, 320-340 ka; Wilson et al., 1986) abutting against, and offset by, the Paeroa Fault. Kapenga Rhyolite domes (Maroa Group) are distributed along the northern and northeastern graben boundary. Ohakuri Formation ignimbrite (ca. 240 ka; Gravley et al., 2007), a non-welded pumice-crystal tuff, occurs as fault-parallel, western and eastern ridges within the basin. Kaingaroa Ignimbrite (230 ka; Houghton et al., 1995) is present in the southern part of the basin, west of the Paeroa Ignimbrite. Overlying the ignimbrites are lake sediments of the Tauranga Group (Leonard et al., 2010), a sequence of finely stratified siltstones, vitric and pumice tuffs, diatomites, sandstones and conglomerates (Brathwaite, 2007). These sediments occur in valleys between blocks of uplifted Ohakuri Formation. Earthquake Flat rhyolitic pyroclastic flows and air fall deposits (64 ka; Wilson et al., 1992) outcrop in the northeastern parts of the basin. Quaternary surface alluvium (that includes Taupo Pumice alluvium) is distributed along structurally-controlled valley floors.

Geothermal systems, as defined by areas of anomalously low resistivity (i.e., <20 Ωm; Figure 2), are spatially associated with the Ngakuru Graben, with surface thermal activity at Waikite, Ngapouri, Te Kopia, Orakeikorako, Atiamuri and Horohoro (Figure 2). All these areas are confined to the western and eastern basin margins, with most (e.g., Waikite, Orakeikorako, Te Kopia, Ngapouri) occurring along or close to the eastern Paeroa Fault.

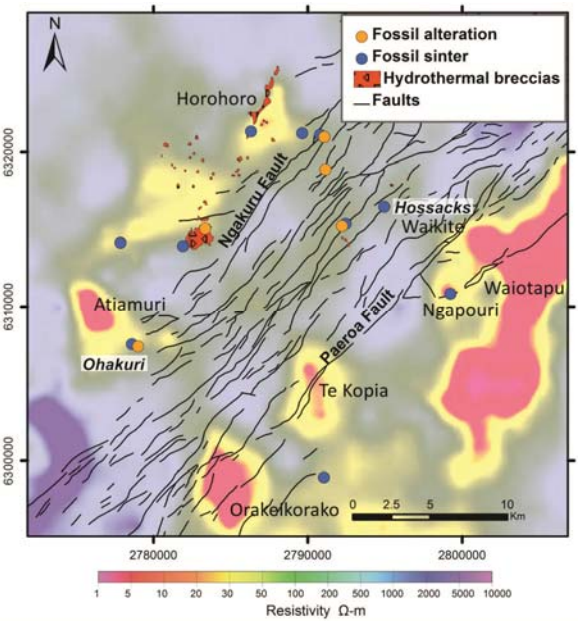


**Figure 2: Electrical resistivity map (detail from Stagpoole and Bibby, 1998) of the Ngakuru Graben with local geothermal systems indicated, along with sites of extinct hydrothermal activity in the form of silica sinter deposits, hydrothermal alteration and eruption breccias.**

Surface mapping of the basin by previous workers (e.g., Brathwaite, 2007, and references therein) has identified sites of extinct geothermal activity (e.g., Ohakuri), in the form of silica sinter deposits, hydrothermal alteration (e.g., zeolite-altered lake sediments) and hydrothermal eruption breccias (Figure 2). Many of these sites occur within or on the edges of conductive zones. These sites, and the few occurring outside conductive zones (e.g., Hossacks; Figures 2 and 3), are all located marginal to the structural basin, at the western, eastern and northern boundaries (Figure 2). Radiometric dating ($^{14}C$) of organic material trapped in sinter sampled from various sites shows that hydrothermal activity has been ongoing on the margins of the Ngakuru Graben for at least the last 34 ± 0.5 ka (Rae et al., in prep).

This work presents the preliminary results of some TOUGH2 modelling where we have attempted to address important questions regarding the temporal and spatial characteristics of geothermal systems associated with a structurally-controlled basin. The questions relate to why hydrothermal activity is restricted to basin margins, why has the location of some of this activity changed or been extinguished and how can we explain the apparent asymmetric focus of hydrothermal activity across the graben. For this work we have queried the influence of basin structural architecture and varying fault permeabilities on fluid flow paths and the location and longevity of geothermal surface discharges.

**Figure 3: Outcrop of silica sinter from an area of extinct geothermal activity at Hossacks, Ngakuru. The sinter is finely to coarsely layered with an apparent thickness of ~2 m.**

## 2. MODEL DESCRIPTION

### 2.1 Fluid Modelling Code

For the models presented in this paper the original version of TOUGH2 (Pruess, 1991) does not have a sufficient working range of temperature and pressure (up to 350°C and 800 bar) so we use an extended version (Kissling, 1995) which uses supercritical fluid properties (to 2000°C and 3000 bar) derived from the NIST formulation (Haar, Gallagher and Kell, 1984). TOUGH2 is a fully implicit integrated finite difference code which solves the (highly nonlinear) time dependent equations for mass and energy conservation in a porous medium, together with appropriate constitutive relationships for the density, enthalpy and viscosity of liquid water and steam. The transport of fluid is described by Darcy's law. These calculations yield the mass and heat flows, and the pressure and temperature distributions within the model domain.

### 2.2 Model setup

The TOUGH2 model domain covering the Ngakuru graben is 30 km wide and 9 km deep and represents a 2D northwest-southeast section across the central graben (Figure 1). We assume that all rocks remain permeable to 9 km. This depth effectively marks the brittle-ductile transition, and is consistent with estimates of its depth within the TVZ derived from earthquake swarms (e.g. Bibby et al., 1995).

The models contain four distinct geological units, as listed in Table 1. The table also gives the permeabilities - all rock types are assumed to have fixed isotropic permeabilities (i.e. horizontal component = vertical component) which remain fixed during the simulations. The fault permeabilities are given in section 3, but we assume that these are typically 5-10x that of the surrounding material – in this case the deep infill (Ingebritsen and Manning, 2010).

The geological layout of the model is shown in Figure 4. The graben is 10 km wide at the surface and narrows to approximately 4.5 km at 9 km depth. The margins of the

graben are defined to the northwest and southeast by a very low permeability unit (or fault zone) dipping at 70° (e.g., Rowland and Sibson, 2001), which extends to the outer lateral boundaries of the model domain. The upper 1 km exterior to the graben, and the upper 2 km within it contain a shallow infill unit consisting of moderate-permeability uncompacted volcanics. Deeper within the graben a lower permeability deep infill unit extends to the base of the model. Faults, where present, lie immediately within the low-permeability margins of the graben and extend from the surface to the base of the model, cutting through the shallower infill material.

We use two different TOUGH2 models (which we label I and II – see Table 2) to calculate the flows and temperature distribution within this region.

The first and main model (I) we use contains approximately 20,000 elements. The elements are varied in size to provide higher resolution within the faults while they remain larger elsewhere in the domain where lower resolution is sufficient. The mesh design ensures that no two neigbouring elements differ in size by more than a factor of two. The element sizes range from 500 m at the lateral boundaries to ~30 m (actually $500/2^4$ m = 31.25 m) within the faults. This has allowed us to represent faults of more realistic width (nominally 150 m ≡ 5 model elements), something which is not practical with a uniform mesh because of the prohibitive number of elements involved.

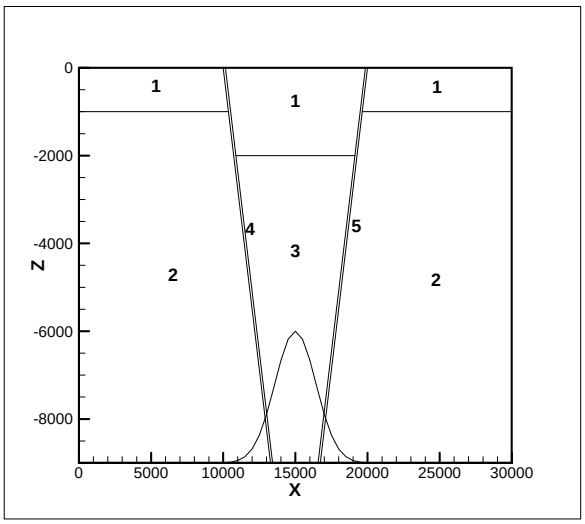


**Figure 4: Geological layout of the model. The numerals indicate, respectively 1) the shallow infill, 2) The exterior unit, 3) the deep infill and 4) & 5) the faults. The curve at the base of the model indicates the form of the heat source. The vertical scale of the figure is exaggerated by approximately 3x.**

The second model (II) uses a uniform mesh containing 27,000 elements, each 100 x 100 m. This complements the model described above as it is used to model the flow of fluid in wide 'permeable zones' (700 m wide) which are too wide to be regarded as faults but nevertheless show interesting (and different) behaviour which is not seen in the main model (I) where the faults are only 150 m wide.

All rocks are assumed to have a porosity of 0.1, thermal conductivity of 2 W/m/K, specific heat capacity of 1000 J/kg/K and a density of 2650 kg/m$^3$.

**Table 1: Rock types and associated permeabilities**

| Rock Type | Permeability (mD) |
|---|---|
| Shallow Infill | 50 |
| Deep Infill | 5 |
| Exterior | 0.001 |
| Faults | see RESULTS section |

For all examples the upper boundary (i.e., the surface) is modelled by a fully liquid-saturated block held at 1 bar pressure and 20°C. As discussed by Kissling and Weir (2005), this adequately represents the situation in the TVZ where only a small fraction of the rainfall is needed to provide the recharge for the geothermal systems. At the lower boundary of all models we apply a constant background heat source of 50 mW/m$^2$ to support a geophysical temperature gradient of 25°C/km. An additional 'geothermal' heat source is used to represent a remnant heat source below the graben (Heise et al., 2010). This has a 'Gaussian' profile, with a peak heat flux of 1000 mW/m$^2$ (comparable to the average heat flux in the TVZ, Bibby et. al., 1995) and a full width at half height of approximately 3.3 km.

Initial conditions for the model are taken to be hydrostatic, corresponding to a conductive temperature profile reaching 245°C at the base of the model (9 km depth). Typically, models were run for between 10 and 200 kyr as this was found to be sufficient to characterise the behaviour of all models.

### 2.3 Model Runs

We present six model runs (A – F; Table 2) of increasing complexity to illustrate the rich variety of phenomena that can occur even in the simple geological models considered here. The permeabilities and other properties of the main units have been given in Table 1 and fault permeabilities for each model are given with the results in Section 3.

**Table 2: Summary of model runs presented.**

| Model, Run | Description |
|---|---|
| I, A | No faults |
| I, B | One right-hand fault (150 m wide) |
| I, C | Two faults of equal permeability (150 m) |
| I, D | Two faults of unequal permeability (150 m) |
| II, E | Two zones of equal permeability (700 m) |
| II, F | Two zones of unequal permeability (700 m) |

## 3. RESULTS

Figure 5 shows the temperature distribution after 200 kyr for model A, where there are no faults at the margins of the graben. In this case a single, rather broad plume of hot fluid forms in the centre of the graben and there are no localised upflows at the margins. The plume is fed by recharge from the surface which descends along the graben walls, gets heated, and subsequently forms the central upflow. The temperature distribution is close to symmetric at this time, but as we later show (Models E and F, figures 9 and 10), instabilities can arise if there is a larger conduit to convey water from the surface to depth.

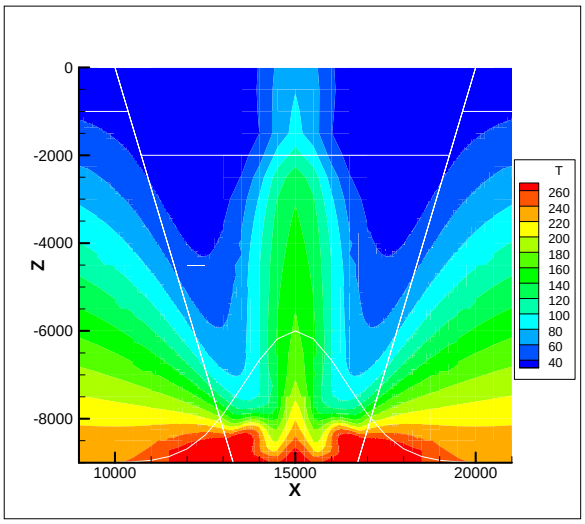


**Figure 5: Temperature distribution after 200 kyr for a model with no faults at the graben margins (Model A). Only the central 12 km of the model are shown in this diagram (and following ones). The white lines delineate the geological units in the model (see Figure 4), and the curve in the lower part of the diagram shows the profile of the deep heat source.**

Figure 6 shows the temperature distribution after 12 kyr, for model B where a single fault is present at the right-hand margin of the graben. The fault is 150 m wide, and the permeability is 500 mD. This clearly acts to convey hot fluid to the surface, where it forms a localised outflow. The source of this hot fluid is initially the pre-existing hot fluid within the graben (as shown in this figure). At later times this fluid is depleted, and recharge consists of cool descending fluid and the same mechanism seen in model A will occur.

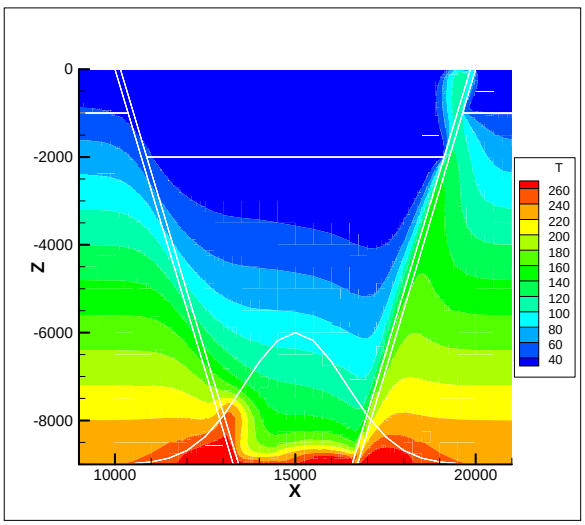


**Figure 6: Temperature distribution after 12 kyr for a model with one fault at the right-hand graben margin (Model B). The higher permeability right-hand fault hosts a strong upflow.**

In figure 7 we show a more complex model (model C), where there are two faults with exactly equal permeabilities (500 mD in this example). Here, the both faults act as conduits for downward flowing cool surface water and a single plume forms in the centre of the graben, similar to model A. In this case however, the recharge is closely associated with the faults, as shown by the deeply penetrating cool water (60°C at ~7 km) and the narrow width of the recharge zones compared to those in model A.

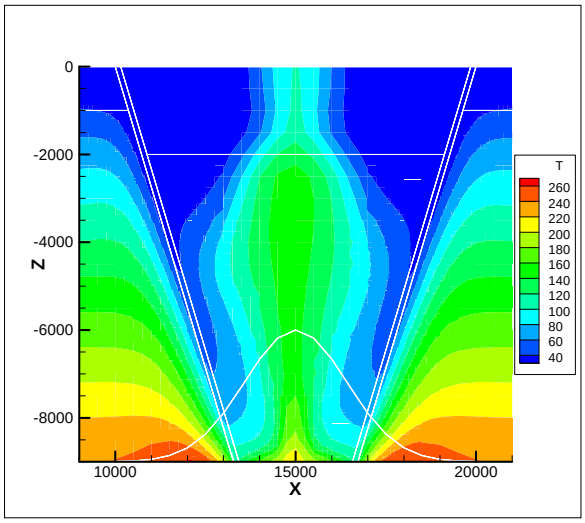


**Figure 7: Temperature distribution after 24 kyr for a model with faults of equal permeability at both left- and right-hand the graben margins (Model C). The presence of two equally high permeability faults leads to two downflows.**

Next, we generalise the model (model D) to again include two faults, but now the permeabilities of these are different. In this case (figure 8), the left- and right-hand fault permeabilities are 400 and 500 mD respectively. An upflow occurs in the highest permeability fault, with a corresponding downflow in the low permeability fault. At the time shown in the figure (26 kyr) the origin of hot outflowing water is changing from the original source water within the graben to heated recharge descending in the left-hand fault. It has not yet been possible to run this model for long enough to determine the long-term behaviour of this system, but cruder models with a uniform mesh suggest that transient central plumes of hot water will form if the fault permeabilities are not sufficient to relay all of the hot fluid to the surface. It is even possible that the hot upflow could oscillate between right- and left-hand faults in this situation.

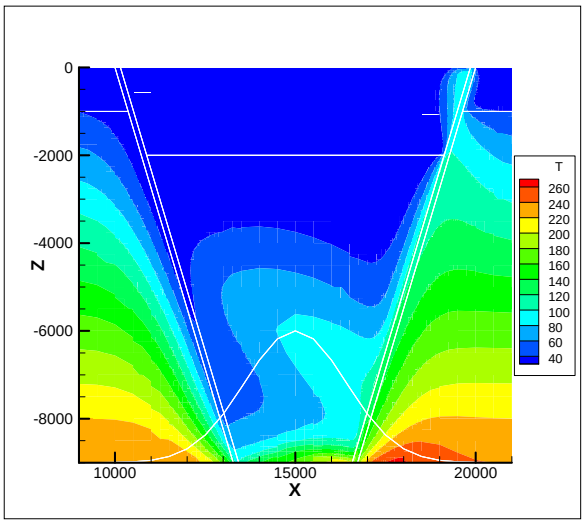


**Figure 8: Temperature distribution after 26 kyr for a model with faults of unequal permeability at both left- and right-hand graben margins (Model D). The highest permeability right-hand fault hosts an upflow and recharge occurs down the lower permeability left-hand fault.**

Figure 9 shows the temperature at 44 kyr from the model E (calculations performed with uniform mesh, see section 2.2), where the faults are replaced by 700 m wide zones of equal high permeability (1000 mD). It is apparent that the flow has become highly asymmetric by this time, with the left-hand zone acting as a downflow and the right-hand zone forming an upflow. The instability is due to a combination of very high permeability in the permeable zones and their large width compared to the previous models. These factors combine to produce a more rapid turnover of fluid within the graben. Also of note is the resolution of details of the flow within the right-hand permeable zone. Here cool downflow and hot upflow occur simultaneously, the former occurring at the foot-wall and the latter at the hanging wall of the permeable zone.

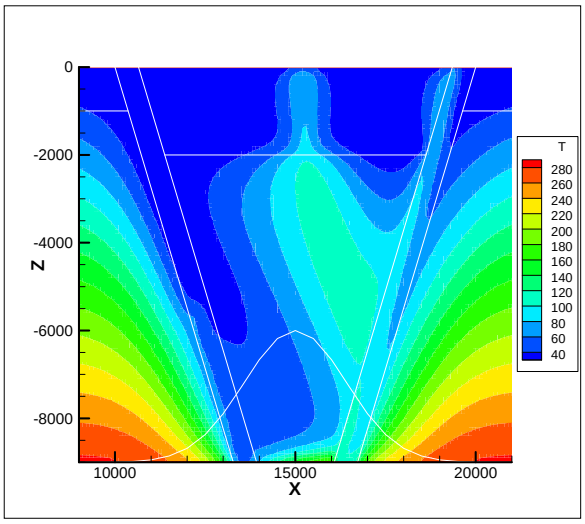


**Figure 9: Temperature distribution after 44 kyr for a model with zones of equal permeability at both left- and right-hand graben margins (Model E). The zones are 700 m wide.**

Lastly, Figure 10 shows the temperature distribution at 24 kyr for a model where the permeable zones have different permeabilities (left = 500 mD, right = 1000 mD). As with model D (figure 8), the lowest permeability fault is on the left-hand side of the graben, and the highest permeability fault is on the right. This shows similar features to those in figure 9, except the upflow now occurs in the lower permeability, left-hand zone. This is in direct contrast to model D, where the upflows occurred in the highest permeability fault.

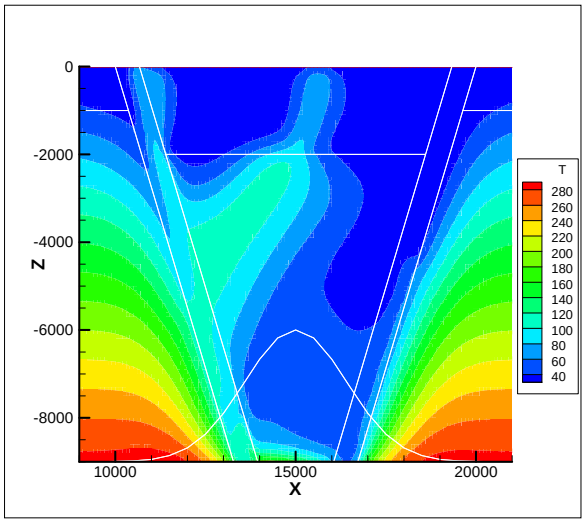


**Figure 10: Temperature distribution after 24 kyr for a model with permeable zones of unequal permeability at the graben margins (Model F). The upflow occurs within the lowest permeability left-hand zone and recharge occurs in the right-hand high permeability zone.**

## 4. DISCUSSION

In this paper we have attempted to address some basic field observations that the focus of geothermal activity in the Ngakuru Graben has been on its margins and is apparently of a transient nature. To do this we have designed an overly simple hydrological model that simulates hydrothermal fluid flow in a graben. However, despite the simplicity our model simulations show remarkably dynamic behaviour that suggests several new mechanisms for the observed localisation of hydrothermal activity and its apparent transiency.

In the simplest model with no faults, only a broad upflow is seen in the central graben. This seems to be too broad to produce any 'local' hydrothermal activity and suggests that some localised permeability is necessary for this to occur. Indeed, further modeling shows that without some additional structure (i.e. narrow high permeability faults) it is not possible for localised upflows to form at the graben margins.

From our small sample of faulted models, we find that warm upflows seem to occur in the highest permeability faults, and downflows in the lower permeability faults. However, for wider permeable zones the reverse seems to be true. The exact relationship of the hot upflows and corresponding cool recharge to the geological setting seems to depend on the nature of the faults (i.e., permeability and width) but is clearly complicated and needs further investigation.

Fault permeabilities are known to vary with time (e.g. Ingebritsen and Manning, 2010) and it has been suggested that they revert to ambient values (i.e., the permeabilities of the host rock) on timescales of years to decades. For the Ngakuru Graben, our models suggest that if this happens with the marginal faults, then large changes in the regional scale hydrology could occur, thus providing a mechanism to explain the presence of fossil hydrothermal systems on both margins of the graben.

For large capacity faults (i.e., wide with high permeability) our models show that the turnover of fluid within the graben can occur in a few 10 kyrs and results in flow instabilities which may cause surface activity to fluctuate between marginal faults across the graben. In this process, brief transient outflows may occur in the centre of the graben away from faults, especially where fault permeabilities are insufficient to relay hot water to the surface. Thus we have a mechanism for the apparent transient nature of hydrothermal activity without invoking a change in the deep heat source or lowering of fault permeabilities through mineralisation.

Further work will add model complexity and test basin fault architecture by querying additional faults in the central parts of the graben and perhaps faults with variable dips.

## 5. CONCLUSIONS

The main conclusions of this work are:

- We have developed a simple fluid flow model of the Ngakuru graben containing four separate geological units to investigate spatial and temporal aspects of hydrothermal activity at the graben margins.
- Even with this simple model, very dynamic regional flows occur, which are strongly dependent on the presence of high permeability faults at the graben margins.
- High permeability faults at the margins of the graben are necessary to the formation of localised hydrothermal activity at those margins. If there are no faults, then no localisation is possible.
- The presence of high permeability faults in the model means that it is not possible to achieve a steady flow/temperature regime within the graben. The instability of the flow provides a mechanism for hydrothermal activity to switch between the margins and also to occur in the central graben.
- For a simple geometry with two faults (150 m wide), upflows occur in the highest permeability fault, and downflows in lowest permeability fault.For wider permeable zones (700 m) upflows occur in the lowest permeability fault, and downflows in the highest permeability fault.
- The circulation of fluid is evident within the wide permeable zones – upflows occur along the hanging wall, and downflows on the foot wall. This is thought to be the result of buoyancy of the hot fluid.
- There is much to explore in the future concerning the role of faults in formation of hydrothermal systems in graben settings such as Ngakuru.

## ACKNOWLEDGEMENTS

We thank L.E. Ramirez who was involved in early discussions of this work.

## REFERENCES

Bibby, H.M., Caldwell, T.G., Davey, F.J. and Webb, T.H.: Geophysical evidence on the structure of the Taupo Volcanic Zone and its hydrothermal circulation. *J. Volcan. Geotherm. Res.* 68, 29-58 (1995).

Brathwaite, R.L.: Geological and mineralogical characterization of zeolites in lacustrine tuffs, Ngakuru, Taupo Volcanic Zone, New Zealand. *Clays and Clay Minerals,* 51, 589-598 (2003).

Gravley, D.M., Wilson, C.J.N., Leonard, G.S. and Cole, J.W.: Double trouble: paired ignimbrite eruptions and collateral subsidence in the Taupo Volcanic Zone, New Zealand. *GSA Bulletin*, 119, 18-30 (2007).

Haar, L., Gallagher, J.S., Kell, G.S.: NBS/NRC Steam Tables, 320 pp. Hemisphere Publishing, New York (1984).

Heise, W., Caldwell, T.G., Bibby, H.M, and Bennie, S.L.: Three- dimensional electrical resistivity image of magma beneath an active continental rift, Taupo Volcanic Zone, New Zealand. *Geophys. Res. Lett.,* 37, (2010). doi:10.1029/2010GK043110.

Houghton, B.F., Wilson, C.J.N., McWilliams, M.O., Lanphere, M.A., Weaver, S.D. and Briggs, R.M., Pringle, M.S.: Chronology and dynamics of a large magmatic system, central Taupo Volcanic Zone, New Zealand. *Geology* 21, 13-16 (1995).

Ingebritsen, S.E. and Manning, C.E.: Permeability of the continental crust: dynamic variations inferred from seismicity and metamorphism. *Geofluids,* 10, 193-205 (2010).

Kissling, W.M.: Extending MULKOM to super-critical temperatures and pressures. *Proc. World Geothermal Congress 1995*, Florence, Italy. 1687 – 1690 (1995).

Kissling, W.M. and Weir, G.J.: The Spatial Distribution of the Geothermal Fields in the Taupo Volcanic Zone, New Zealand. *J. Volcan. Geotherm. Res.* 145, 136-150 (2005).

Leonard, G.S., Begg, J.G. and Wilson, C.J.N. (compilers): Geology of the Rotorua Area. *Inst. of Geol. & Nucl. Sci.* 1:250 000 geological map 5. 1 sheet + 102 p. Lower Hutt, New Zealand. GNS Science (2010).

Pruess, K.: TOUGH2 – A General Purpose Numerical Simulator for Multi-phase Fluid and Heat Flow. Report LBL-29400. Lawrence Berkeley Laboratory, 70pp (1991).

Rowland, J.V. and Sibson, R.H.: Extensional kinematics within the Taupo Volcanic Zone, New Zealand: soft-linked segmentation of a continental rift system. *N.Z.J. Geol. Geoph.* 44, 271-283 (2001).

Stagpoole, V.M. and Bibby, H.M.: Electrical resistivity map of the Taupo Volcanic, New Zealand; nominal array spacing 500 m, 1:250 000, version 1.0. Institute of Geological & Nuclear Sciences geophysical map 11.

Institute of Geological & Nuclear Sciences Ltd., Lower Hutt, N.Z. (1998).

Villamor, P. and Berryman, K.: A late Quaternary extension rate in the Taupo Volcanic Zone, New Zealand, derived from fault slip data. *N. Z. J. Geol .Geoph.* 44, 243-269 (2001).

Wilson, C.J.N., Houghton, B.F. and Lloyd, E.F.: Volcanic history and evolution of the Maroa-Taupo area, central North Island. *In* Smith, I.E.M. *ed*. Late Cenozoic volcanism in New Zealand. *Royal Soc. N.Z. Bull.* 23, 194-223 (1986).

Wilson, C.J.N., Houghton, B.F., Lanphere, M.A. and Weaver, S.D.: A new radiometric age estimate for the Rotoehu Ash from Mayor Island volcano, New Zealand. *N. Z. J. Geol .Geoph.* 35, 371-374 (1992).